The Effective Use of Aerodynamic Balance on Control Surfaces

L. E. ROOT*

Douglas Aircraft Company, Inc.

SUMMARY

This paper is concerned with (a) an analysis of wind-tunnel data obtained from a 2-ft. constant chord control surface model constructed so that the separate effects of variation in aerodynamic balance overhang and movable surface nose shape could be obtained, and (b) the presentation of design methods leading toward the effective use of aerodynamic balance on control surfaces. The basic airfoil section used is an NACA 0012 modified to 10.7 per cent maximum thickness by 12 per cent chord extension and straight-sided afterbody. These modifications were made in accordance with 1935 results from DC-2 flight tests which specifically indicated that flat-sided rudders or elevators were less subject to flow conditions causing undesirable oscillations, particularly when control forces had been substantially reduced through the use of aerodynamic balance. The nature of the overhanging balance effectiveness in reducing hinge moments is illustrated by presenting representative pressure distributions over a surface with and without balance at various angles.

Using theoretic control surface parameters for simply hinged flaps as a basis, hinge-moment data from the model were analyzed to obtain empiric factors that correct for variations in aerodynamic balance and nose shape. Parameters are obtained for use in estimating three-dimensional control surface effectiveness and hinge moments with a degree of accuracy corresponding to the similarity of airfoil sections taken along the span of any specific control surface to the section tested, particularly with respect to movable surface shape. This method of calculating hinge moments has been checked by measurements on scale airplane models and was found to be reasonably accurate considering differences in hinge-line locations. Upon the basis of hinge-moment tests on sharp (A), medium (B), and blunt (C) noses, an intermediate shape, (B + C)/2, was chosen for design use. Comparison of control surface factors for this nose shape obtained from scale airplane model tests and from the basic model show good agreement.

With particular respect to air-transport operation, an important factor affecting the design of the movable control surface section is the degree to which the balance nose is subject to critical icing when the surface is held at a trim angle, such as in the case of a rudder after engine failure. From 1937 tests in the Goodrich ice tunnel using the 2-ft. chord model, an approximate relationship between balance nose shape and critical ice formation was suggested. Application of this limit to the (B + C)/2 nose-shaped rudders on present multiengined transports at best rate of climb with full asymmetric power indicates that the required rudder angles are not critical to dangerous icing conditions.

Additional factors affecting the choice of aerodynamic balance are discussed, and practical design limits applicable to elevators are given. From the basic wind-tunnel data, relationships of maximum up-travel, horizontal surface stalling, and free-control longitudinal stability to variation in aerodynamic balance and nose shape are determined. Application of these limits to typical airplane designs, in relation to the amount of hinge-moment reduction desired and the amount of balance recommended, shows the basic difficulty of reducing elevator control forces to acceptable magnitude and at the same time of providing enough elevator control for landing without exceeding the design limits.

To illustrate the use of aerodynamic balance on control surfaces, representative horizontal and vertical mean airfoil sections for eight Douglas airplanes are presented. Both the shape and amount of balance are clearly shown, as well as hinge location, maximum travel, control surface gap, and modifications to the basic airfoil. It is emphasized that proportionality of plan form and section will contribute to the more effective use of aerodynamic balance. To obtain maximum hinge-moment reduction for a given degree of unporting, it is necessary to avoid plan-form irregularities and movable control surface area aft of the hinge line which cannot be effectively balanced.

Presented at the Summer Annual Meeting, I.A.S., Los Angeles, July 27–28, 1944.

* Chief, Aerodynamics Section, El Segundo Plant.

INTRODUCTION

THE SATISFACTORY DESIGN of control surfaces on an airplane has always presented a fundamentally difficult aerodynamic problem, particularly with respect to control force reduction. Although symmetric overhang-type aerodynamic balance has been used on many movable surface designs, this use has been all too frequently associated with undesirable cut-and-try processes during experimental flight tests leading toward an acceptable arrangement. Such was the experience of the Douglas Aircraft Company, Inc., during the final development of the Model DC-2 transport control surfaces in the first half of 1935. Upon the basis of flight-test results obtained with a number of variations in elevator and rudder plan form and section on the DC-2 airplane, a few basic principles of control surface design were indicated. As a step toward further clarification of these principles, extensive wind-tunnel tests were conducted in the 10-ft. circular wind tunnel at GALCIT in the early part of 1936 on a large-scale control surface model so constructed that the separate effects of variation in overhang and balance nose shape could be obtained. The results from these wind-tunnel tests, used in combination with the DC-2 flight experience, have effectively contributed to the successful design of control surfaces on Douglas airplanes.

This material is offered with the full realization that there are many ways to design control surfaces which are entirely satisfactory but do not necessarily incorporate the features presented. With variation in airplane size, it is possible that optimum aerodynamic balancing of control surfaces is not always necessary, although its consistent use will undoubtedly result in the most efficient arrangement for a large airplane, particularly with respect to weight reduction. In the case

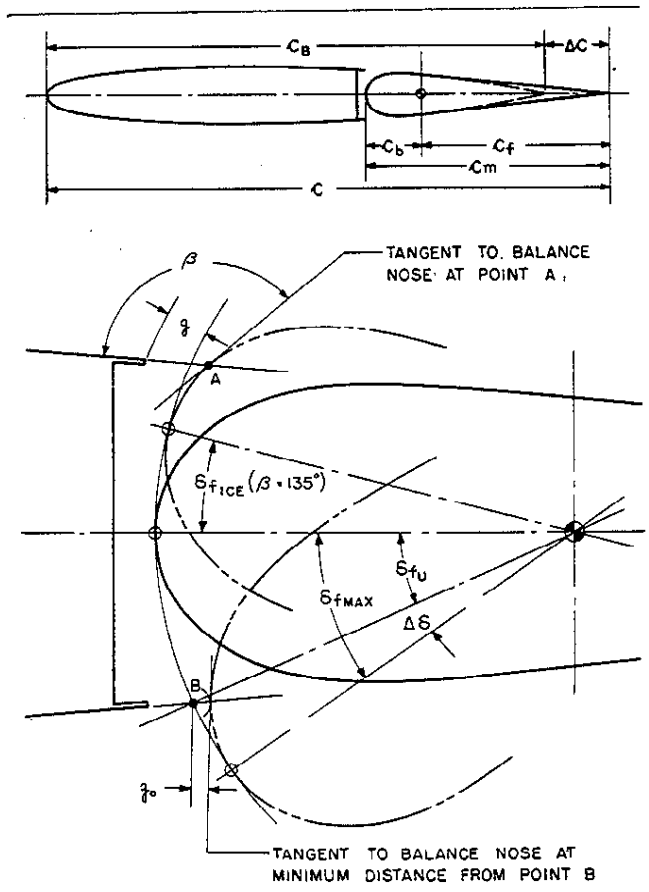

FIG. 1. Definition of control surface chords, gaps, and angles associated with the use of aerodynamic balance.

of smaller airplanes, particularly those restricted in dimensions, free-control stability considerations may predominate, thus limiting the use of proportional aerodynamic balance to partial control surface span. Bearing in mind the compromising nature of control surface design and the many associated difficulties, this paper is presented with the thought that Douglas design practice may be of general interest.

SYMBOLS

Chords, Gaps, and Angles (See Fig. 1)

- c = chord of control surface airfoil section
- $\bar{c}$ = mean geometric chord
- c_f = chord of movable control surface section aft of hinge line
- c_B = chord of basic control surface airfoil section before chord extension
- Δ_c = chord of extension to give modified airfoil section with straight-sided afterbody
- c_b = chord of movable control surface airfoil section ahead of hinge line
- c_m = chord of movable control surface airfoil section including balance ($c_b + c_f$)
- c_b/c_f = aerodynamic balance or overhang of movable control surface section
- c_h/c_m = hinge-line location of movable control surface section from balance nose leading edge
- g = minimum clearance gap between fixed and movable control surface sections
- g_0 = overtravel gap for movable control surface section
- x = chordwise station of airfoil section
- δ_f = movable control surface angle in degrees with respect to fixed surface
- δ_{f_u} = movable control surface angle in degrees where balance nose leading edge starts to project or unport beyond airfoil contour
- $\delta_{f_{max.}}$ = angle in degrees at which movable control surface hits mechanical stop
- $\Delta\delta$ = angular overtravel in degrees, ($\delta_{f_{max.}} - \delta_{f_u}$)
- β = angle in degrees between airfoil contour and line tangent to balance nose at point of intersection with airfoil
- $\delta_{f_{ice}}$ = movable control surface angle in degrees beyond which disturbing ice formations are likely to occur ($\delta_{f_{ice}}$ is taken when $\beta = 135°$)
- α = control surface angle of attack for finite span in degrees
- α_0 = control surface angle of attack for infinite aspect ratio in degrees
- a_0 = slope of control surface lift curve for infinite aspect ratio, $2\pi\eta$, radian measure (in text, $\eta = 0.875$)
- ψ = angle of yaw in degrees

Coefficients and Parameters

- C_L = control surface lift coefficient, (L/qS)
- c_l = airfoil section lift coefficient, (l/qc)
- C_H = movable control surface hinge-moment coefficient, ($H/q\bar{c}_f S_f$)
- c_h = movable control surface section hinge-moment coefficient, (h/qc_f^2)
- $C_{L\alpha} = \partial C_L/\partial\alpha$
- $c_{l\alpha} = \partial c_l/\partial\alpha$
- $C_{L\delta} = \partial C_L/\partial\delta$
- $C_{H\alpha} = \partial C_H/\partial\alpha$
- $c_{h\alpha} = \partial c_h/\partial\alpha$
- $C_{H\delta} = \partial C_H/\partial\delta$
- $c_{h\delta} = \partial c_h/\partial\delta$
- $\eta_\alpha, \eta_\delta, \eta_\lambda$ = empiric control surface hinge moment and effectiveness factors used to correct for variations in balance nose shape and overhang
- AR = geometric aspect ratio, (b^2/S)
- AR_e = effective aspect ratio
- p = lift curve slope reduction factor without end plates
- r = lift curve slope correction factor with end plates

Subscripts

- C_L, c_l, δ = variables held constant during differentiation
- f = movable control surface aft hinge line
- m = movable control surface including overhang
- b = balance or overhang
- r = rudder, chord aft hinge line
- e = elevator, chord aft hinge line
- W = wing
- H = horizontal control surfaces
- V = vertical control surfaces

Capital letters used in designating forces, moments, and their coefficients and derivatives indicate finite aspect ratio characteristics, while lower case letters indicate section characteristics.

CHOICE OF CONTROL SURFACE AIRFOIL SECTION

In view of optimum lifting characteristics shown for the NACA 0012 section[1] this airfoil was chosen as basic for control surface use and modified by a 12 per cent chord extension and straight-sided afterbody as shown in Fig. 2. Ordinates for this modified airfoil section are given in Table I. Although the maximum thickness was thus reduced to 10.7 per cent based on the extended chord, it was considered that the desirable aero-

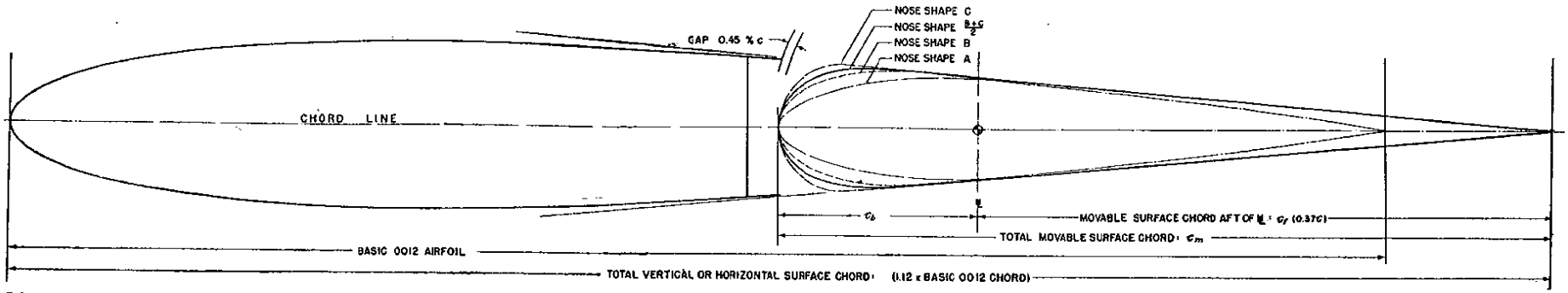

FIG. 2 : THE DEVELOPMENT OF A SUITABLE CONTROL SURFACE AIRFOIL SECTION

METHOD OF AIRFOIL CONSTRUCTION: THE NACA 0012 AIRFOIL SECTION IS MODIFIED BY EXTENDING THE CHORD 12% AND DRAWING STRAIGHT LINES FROM THIS EXTENDED POINT TANGENT TO THE BASIC AIRFOIL AT THE 60% CHORD POINT. THICKNESS BASED ON THE NEW CHORD IS 10.7%. FOR CONVENTIONAL RATIOS OF MOVABLE TO FIXED SURFACES, THE ELEVATOR OR RUDDER WILL HAVE STRAIGHT SIDES AFT OF THE H.L.

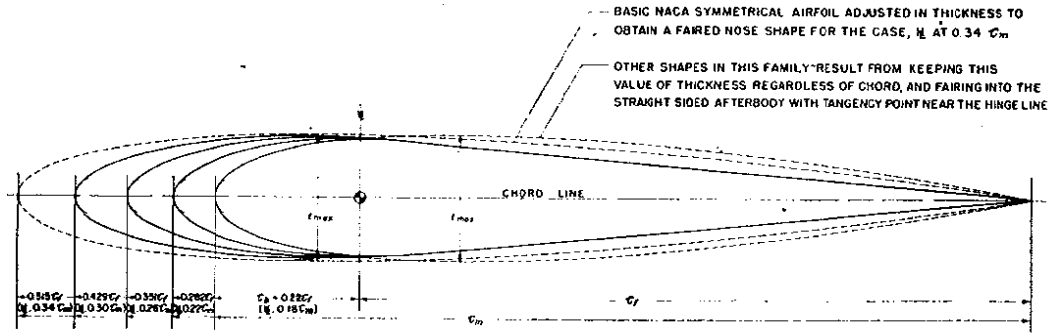

(a) MOVABLE CONTROL SURFACES WITH NOSE SHAPE A

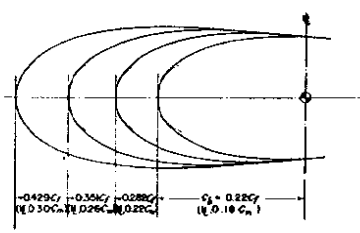

(b) NOSE SHAPE B

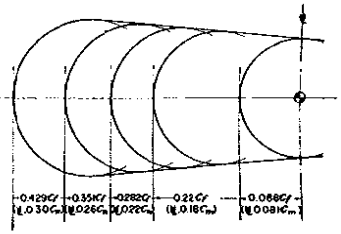

(c) NOSE SHAPE C

FIG 3 : SYSTEMATIC VARIATION OF AERODYNAMIC BALANCE AND NOSE SHAPE

METHOD OF BALANCE NOSE CONSTRUCTION

NOSE SHAPE A USING THE FUNDAMENTAL NACA SYMMETRICAL AIRFOIL THICKNESS DISTRIBUTION WITH MAXIMUM THICKNESS AT 30% CHORD, BASIC NOSE SHAPE A IS OBTAINED WITH TOTAL MOVABLE SURFACE CHORD AS A BASIS. ONLY THE ORDINATES FORWARD OF 30% CHORD ARE REQUIRED TO FAIR INTO THE STRAIGHT SIDED AFTERBODY. MAXIMUM THICKNESS IS ADJUSTED FOR THE VARIOUS NOSES TO OBTAIN A POINT OF TANGENCY WITH THE STRAIGHT SIDES AS CLOSE TO THE HINGE LINE AS POSSIBLE. FOR EXAMPLE, IN THE CASE WITH THE H.L. AT 0.26 Cm, THE TANGENCY POINT IS AT 0.28 Cm. FOR THE SHORTER NOSES, SOME FAIRING ADJUSTMENT IS NECESSARY NEAR THE HINGE LINE.

NOSE SHAPE C CONSTRUCTION OF THIS SHAPE IS OBTAINED BY FORWARD EXTENSION OF THE STRAIGHT SIDES TANGENT TO A LEADING EDGE CIRCLE OF MAXIMUM RADIUS.

NOSE SHAPE B AN INTERMEDIATE NOSE BALANCE SHAPE IS OBTAINED BY USING ORDINATES HALF WAY BETWEEN THOSE FOR NOSES A AND C. SOME FAIRING ADJUSTMENT IS REQUIRED NEAR THE TANGENCY POINT AS CAN BE SEEN ABOVE IN FIG 3b. TANGENCY POINT WITH THE STRAIGHT SIDES FOR THIS NOSE IS MIDWAY BETWEEN THOSE FOR NOSE A AND NOSE C.

NOSE SHAPE USED IN DESIGN AERODYNAMIC BALANCE NOSE SHAPE USUALLY EMPLOYED IN DOUGLAS DESIGNS IS ONE TERMED $\frac{B+C}{2}$, OR INTERMEDIATE BETWEEN THE SHAPES B AND C, DESCRIBED ABOVE.

ORDINATES IN PERCENT OF AIRFOIL CHORD	
STATION	ORDINATES
.000	.000
1.116	1.691
2.232	2.335
4.460	3.174
6.700	3.750
8.930	4.181
13.390	4.772
17.850	5.123
22.320	5.304
26.780	5.359
35.710	5.181
44.640	4.726
53.570	4.074
62.500	3.271
100.000	.000
L.E.R.	1.41

STRAIGHT TAPER FROM APPROXIMATELY 60% CHORD TO TE

TABLE I : ORDINATES FOR NACA 0012 AIRFOIL MODIFIED TO 10.7% THICKNESS

ORDINATES IN PERCENT OF TOTAL MOVABLE SURFACE CHORD	
STATION	ORDINATES
1.25	3.633
2.50	4.931
5.00	6.371
7.50	7.132
10.00	7.454
15.00	7.420
20.00	7.048
100.00	.000
L.E.R.	5.3

TABLE II : ORDINATES FOR $\frac{B+C}{2}$ NOSE SHAPE

dynamic characteristics of the 0012 airfoil were maintained for the most part.

The afterbody modification to straight sides was a result of DC-2 flight-test experience with a number of control surface modifications. With flat sides, for example, the DC-2 rudder exhibited a marked reduction in the magnitude of oscillations, particularly in disturbed air. As a verification of this effect, a "bulged" rudder with convexity purposely overemphasized gave an extreme increase in surface oscillations. Since this same phenomenon occurred in the case of an elevator on the DC-2, it was definitely indicated that movable control surface sections should be modified to have straight-sided afterbodies for design use if the possibility of peculiar characteristics were to be minimized. The 12 per cent chord extension was therefore chosen so that the amount of afterbody usually employed for a movable control surface would have flat sides aft of the hinge line.

Basic Wind-Tunnel Tests

GALCIT Model and Tests

Using the symmetric airfoil section described above, a 2-ft. chord, 6-ft. span model with end plates was constructed so that the movable surface balance nose shape and amount of overhang could be systematically varied with one hinge-line position of 63 per cent c. The range of adjustments is illustrated in Fig. 3 where the method of construction for the different nose shapes is described. Balance noses are designated as sharp (nose shape A), medium (nose shape B), and blunt (nose shape C). Details of the model are shown in Fig. 4. Removable cover plates made it possible to maintain a constant gap of 0.45 per cent c with changes in balance overhang.

The model was rigged in the GALCIT 10-ft. wind tunnel as shown in Fig. 5 so that lift and drag could be measured in the normal manner and hinge moments could be obtained directly from the pitching moment balance. For each run the fixed surface was set at a given angle of attack and the flap rotated through a series of positions.

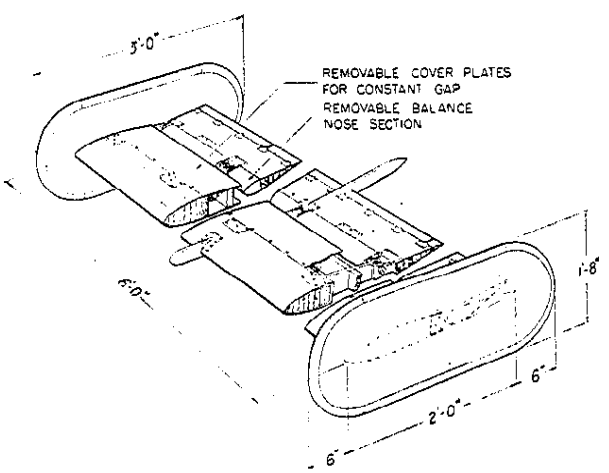

FIG. 4. Basic 2-ft. chord model used to obtain the effects of variation in movable control surface nose shape and aerodynamic balance. Test Reynolds Number 2.2×10^6.

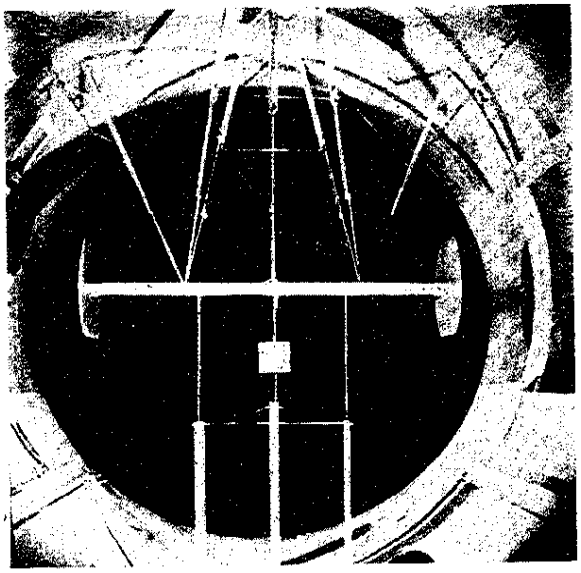

FIG. 5. Basic 2-ft. chord control surface model rigged in GALCIT 10-ft. wind tunnel.

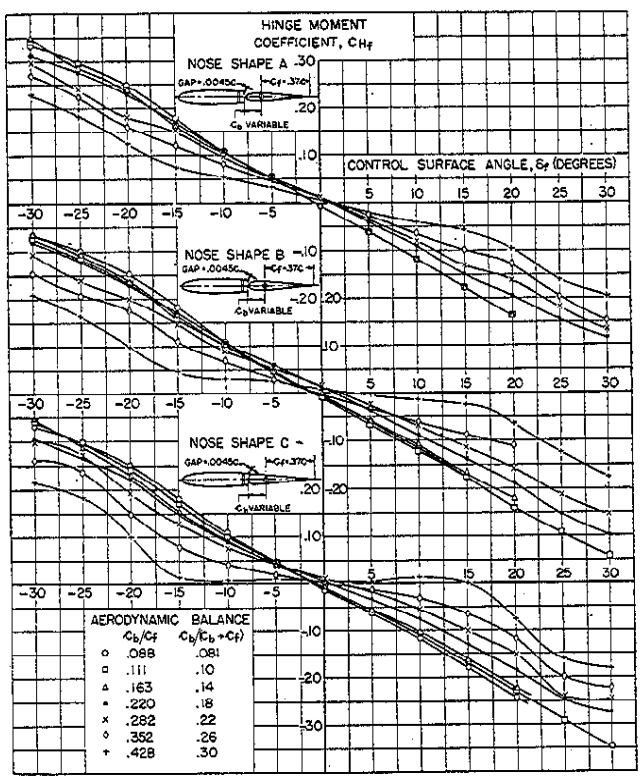

FIG. 6. Basic hinge moment curves at $\alpha = 0°$ for model of Fig. 4 with changes in aerodynamic balance and nose shape.

No attempt was made to correct data for tunnel-wall interference in view of the use of end plates, since interference corrections for a wing with end plates were not known. Corrections were made, however, for tare moment. Tests were conducted at a wind speed of 132 m.p.h. corresponding to a Reynolds Number based on total chord of 2,200,000. Hinge-moment data ob-

tained from the several balance nose shapes and amounts of overhang were plotted in the form shown in Fig. 6 ($\alpha = 0°$) for angles of attack of 0°, 5°, 10°, 15°, and 20°.

Control Surface Icing Tests

Through the courtesy of The B. F. Goodrich Company, refrigerated wind-tunnel tests were made in June, 1937, on the 2-ft. chord control surface model of Fig. 4 using various balance nose shapes and amounts of overhang. Since the object of these tests was to determine where and how ice would form on the various movable surface noses, wax impressions were taken where ice became of appreciable thickness and plaster casts were made. By starting each run at the same temperature and keeping the duration constant, comparisons between various nose ice formations could be made.

Photostats of the plaster casts have been reduced in size and are represented in Fig. 7 for $\alpha = 0°$. Although it was originally intended to duplicate ice formations obtained on the several nose shapes and to measure hinge moments in the wind tunnel, this was never done. The results from the ice tunnel, therefore, must necessarily remain qualitative in nature.

Control Surface Pressure Distribution

In connection with the structural design of one particular airplane, it was necessary to obtain representative pressure distributions over the vertical surface with and without rudder aerodynamic balance. Wind-tunnel tests were conducted at GALCIT on a complete scale model equipped to measure pressures on fin and rudder at various angles of rudder deflection and yaw. Pressure distributions for the mean vertical surface airfoil section are shown in Fig. 8 for a test Reynolds Number of 870,000 based on the above chord. These data are presented as a matter of interest in showing the effect of aerodynamic nose balance upon the pressure distribution over a representative control surface section.

Analysis of Data

Theory

The equations for the lift and hinge-moment characteristics of a control surface with finite aspect ratio under the assumptions of the lifting-line theory and for an elliptic span loading may be written in the following differential form:

$$dC_L = C_{L_\alpha}\, d\alpha + C_{L_\delta}\, d\delta \tag{1}$$

$$dC_H = C_{H_\alpha}\, d\alpha + C_{H_\delta}\, d\delta \tag{2}$$

From Eqs. (1) and (2)

$$C_{H_\alpha} = \left(\frac{dC_H}{dC_L}\right)_\delta C_{L_\alpha} = \left(\frac{dc_h}{dc_l}\right)_\delta C_{L_\alpha} \tag{3}$$

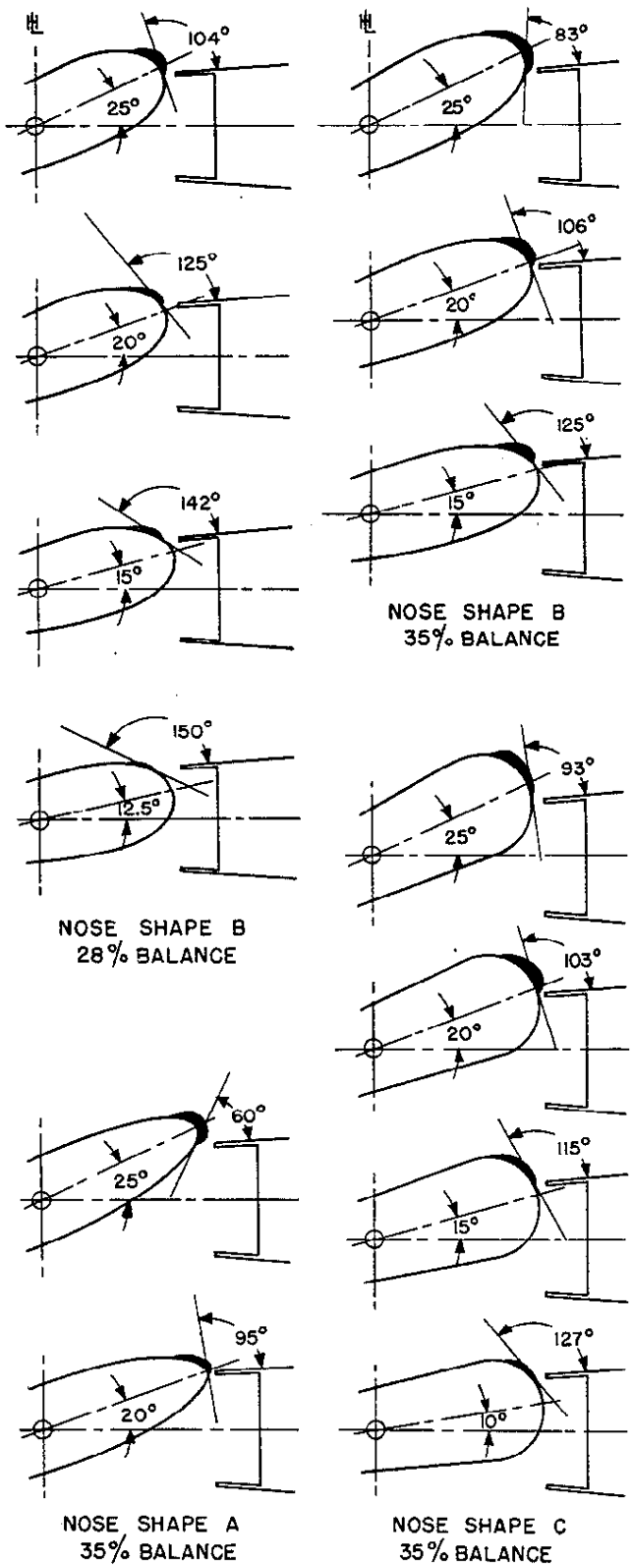

FIG. 7. Ice formations on a movable control surface with variations in aerodynamic balance and nose shape. Tests were made in the Goodrich ice tunnel using model of Fig. 4 at zero angle of attack.

From Eq. (2)

$$C_{H_\delta} = (dC_H/d\delta) - C_{H_\alpha}(d\alpha/d\delta) \tag{4}$$

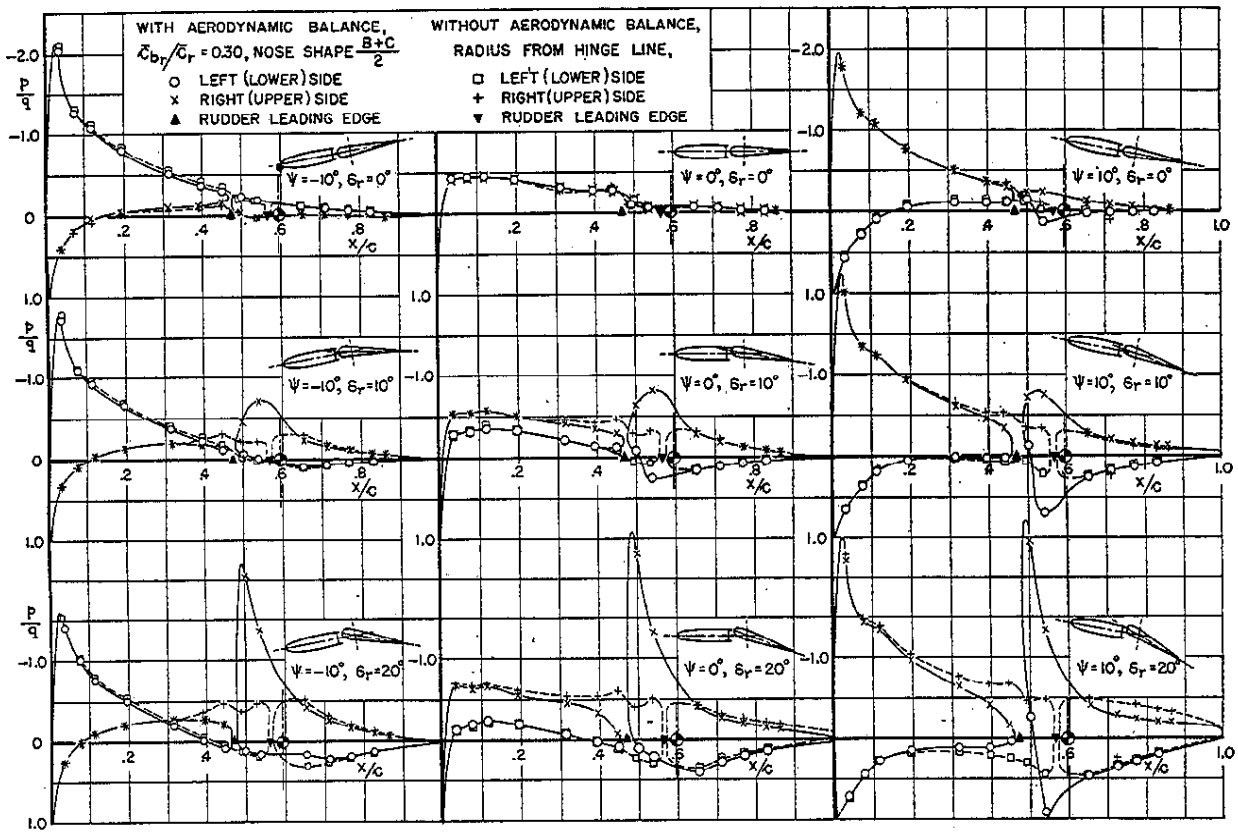

FIG. 8. Representative pressure distributions obtained from the GALCIT 10-ft. wind tunnel on the mean airfoil section of a vertical surface at various angles of yaw and rudder deflection with and without aerodynamic balance. Airfoil section and hinge locations shown in Fig. 18, Airplane No. 2. Test Reynolds Number 870,000. Gap = 0.0023C.

Substituting Eq. (3) in Eq. (4) and fixing $d\alpha/d\delta$ by the condition that C_L be constant during the variation in α and δ, Eq. (4) becomes,

$$C_{H_\delta} = \left(\frac{dc_h}{d\delta}\right)_{cl} - \left(\frac{dc_h}{dc_l}\right)_\delta \left(\frac{d\alpha}{d\delta}\right)_{cl} C_{L_\alpha} \qquad (5)$$

where

$$(dC_H/d\delta)_{C_L} = (dc_h/d\delta)_{cl} \qquad (6)$$

under the above assumptions.

Empiric Correction Factors

Using the lift and hinge-moment data from the basic wind-tunnel model, necessary cross plots were made and slopes were measured so that empiric correction factors could be determined for variations in aerodynamic balance and nose shape. These slopes were read between the limits $-10° < \delta < +10°$ and $0° < \alpha < +10°$. The correction factors, designated as η_α, η_δ, and η_λ, are applied to the section coefficients from thin-airfoil theory in the following manner:

$$(d\alpha/d\delta)_{C_L} = \eta_\lambda (d\alpha/d\delta)_{cl} \qquad (7)$$

$$C_{H_\alpha} = \eta_\alpha (dc_h/dc_l)_\delta C_{L_\alpha} \qquad (8)$$

$$C_{H_\delta} = \eta_\delta \left(\frac{dc_h}{d\delta}\right)_{cl} - \eta_\lambda \left(\frac{d\alpha}{d\delta}\right)_{cl} \left[\eta_\alpha \left(\frac{dc_h}{dc_l}\right)_\delta C_{L_\alpha}\right] \qquad (9)$$

The section parameters, $(d\alpha/d\delta)_{cl}$, $(dc_h/dc_l)_\delta$, and $(dc_h/d\delta)_{cl}$ are obtained from Fig. 10. Correction factors are given in Fig. 9 for various nose shapes and amounts of overhang. Since these factors are independent of aspect ratio only under the assumptions of the lifting-line theory and for an elliptic span loading, their use can be considered to give strictly accurate results only for the control surface configuration tested. Design experience, however, has indicated that η_α, η_δ, and η_λ may be used with reasonable accuracy over the normal range of aspect ratios for control surfaces having the airfoil section of Fig. 2 and proportional plan form.

As an indication of the accuracy that can be expected, comparisons were made between calculations and scale airplane model tests where movable control surface hinge moments were measured. Agreement is shown in Fig. 11 where calculated values of C_{H_α} and C_{H_δ} are compared with those obtained from complete model empennages with control surface aspect ratios ranging from 1.5 to 5.0. It is indicated that a reasonable approximation of hinge-moment parameters may be expected using the factors of Fig. 9. C_{L_α} for the finite-span model surfaces was obtained from the relation

$$C_{L_\alpha} = p\left[\frac{a_0}{1 + (ra_0/\pi AR_e)}\right]\frac{\pi}{180} \qquad (10)$$

AR_e, p, and r depend upon the type of control surface design as follows:

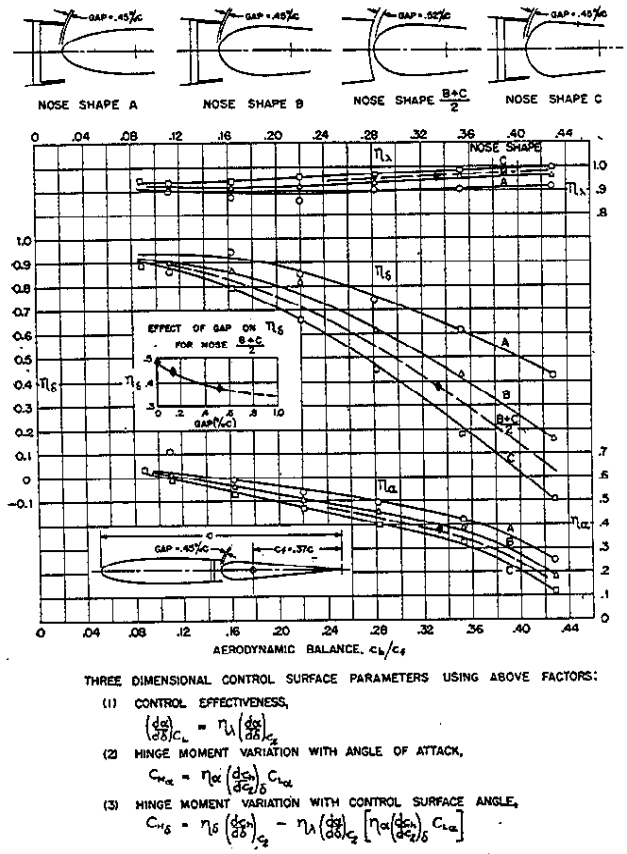

FIG. 9. Factors η_α, η_δ, and η_λ used for obtaining control surface hinge moment and effectiveness parameters when aerodynamic balance and nose shape are varied.

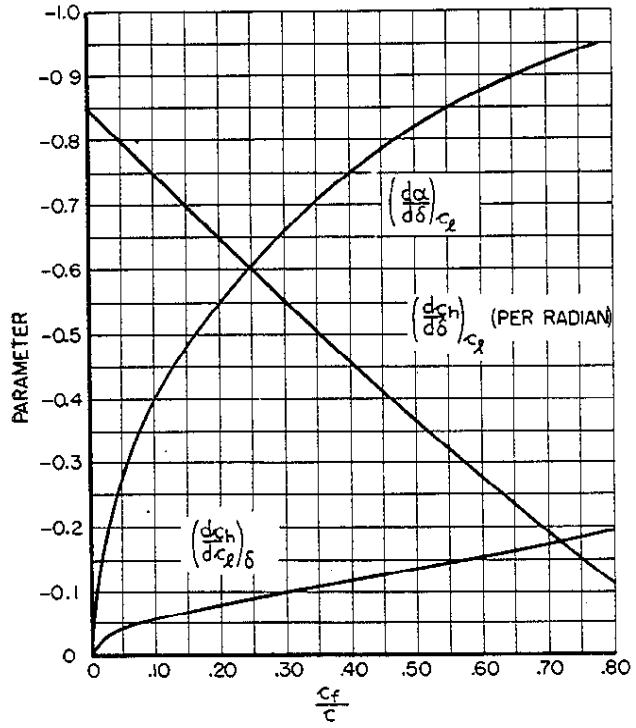

FIG. 10. Theoretic control surface parameters for simply hinged flaps. Multiplicative factors η_α, η_δ, and η_λ give corrected parameters for the aerodynamic balance variations shown in Fig. 3 using the airfoil section of Fig. 2.

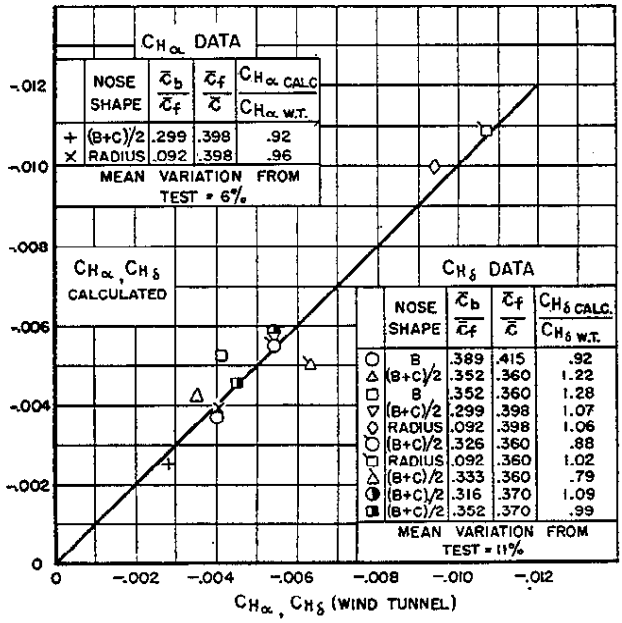

FIG. 11. Comparison of hinge moment parameters $C_{H\alpha}$ and $C_{H\delta}$ obtained from calculations and wind-tunnel tests showing the accuracy that may be expected using the factors η_α, η_δ, and η_λ.

$AR_{H_e} = AR_H$, p variable with single vertical surfaces

$AR_{H_e} = AR_H$, r variable, $p = 1.0$ with double vertical surfaces

$AR_{V_e} = 1.55\, AR_V$, $p = 1.0$ with single vertical surfaces

$AR_{V_e} = AR_V$, $p = 1.0$ with double vertical surfaces

Parameters p and r are found in Fig. 4 of reference 2.

The nose shape adopted for design and used in most cases on the various model control surfaces was intermediate between shapes B and C, designated as (B + C)/2. This shape is shown in Fig. 2 with ordinates given in Table II. Tests on the basic model (Fig. 4) were made with this nose shape and one value of aerodynamic balance, $\bar{c}_b/\bar{c}_f = 0.33$.

Correction factors for other values of overhang are taken intermediate between those for shapes B and C as shown in Fig. 9. Agreement between this interpolated curve and actual test points on complete models with control surfaces having nose shape (B + C)/2 is shown in Fig. 12. Considering variations in hinge-line location, the comparison is reasonably good. In determining η_α and η_δ from wind-tunnel tests on the complete models, it was assumed that the dynamic pressure at the tail equaled that in the free stream.

DESIGN FACTORS AFFECTING THE CHOICE OF AERODYNAMIC BALANCE

Control Forces

Obviously, the primary purpose for using aerodynamic balance on movable control surfaces is to reduce control forces. Through choice of nose shape and amount of balance overhang, a considerable range of hinge moment adjustment is available, although defi-

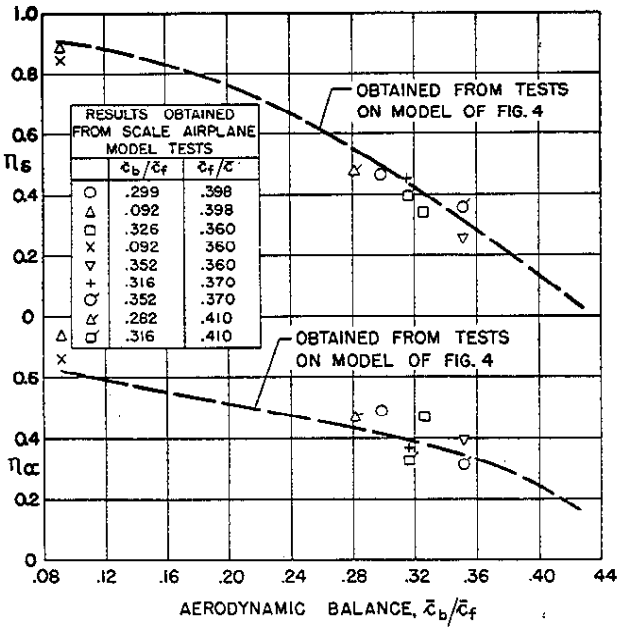

FIG. 12. Comparison of hinge moment factors η_α and η_δ obtained from tests on the model of Fig. 4 and tests on scale airplane models having control surfaces with balance nose shape (B+C)/2.

nitely restricted by other control surface design requirements. In the case of modern airplanes characterized by relatively wide speed ranges, it will undoubtedly be impossible to solve all the control-force problems satisfactorily through the use of aerodynamic balance alone. Some hinge-moment reduction can be effected, however, thus resulting in a more efficient control system by virtue of lighter design loads. In the case of an extremely large aircraft, hinge-moment reduction will add to flight safety in the event of power boost failure, since the pilot can more easily control the airplane directly through his own strength.

As a means of presenting what can be accomplished, three representative airplane designs with gross weights varying from 15,000 to 60,000 lbs. have been studied with respect to elevator stick force per unit normal acceleration in pull-outs. For each design the horizontal surfaces were chosen to satisfy the longitudinal stability and control requirements of the particular case, using the modified airfoil section of Fig. 2 and proportional horizontal surface plan form. Elevator aerodynamic balance overhang and nose shape were then varied, giving the force changes shown in Fig. 14. These changes were computed using the empiric correction factors of Fig. 9, a common c.g. location of 25 per cent M.A.C. (mean aerodynamic chord), and sea-level altitude. Based upon recent control-force requirements, values of stick force per unit acceleration should be 10, 30, and 45 for the one-, two-, and four-engined cases, respectively. Although inspection of each example presented in Fig. 14 shows that the above-required values of stick force per unit acceleration could be obtained with some combination of elevator nose shape and balance overhang, certain design limitations exist and will be discussed below.

The aerodynamic balance designs recommended for the various cases incorporate the intermediate nose shape (B + C)/2, with values of $\bar{c}_b/\bar{c}_f = 0.33$, 0.33, and 0.37. From Fig. 14 these balance combinations give stick forces under acceleration of 20, 30, and 110 lbs. per g, thus indicating that elevator control forces are in excess of requirements in the first and third cases. Since a common c.g. position of 25 per cent M.A.C. may not represent final comparative normal loading conditions for one-, two-, and four-engined airplanes, the relative magnitude of these forces may change. It may be concluded from Fig. 14, however, that difficulty can be expected in meeting elevator control-force requirements for all cases through the use of balance overhang alone. Nevertheless, the effectiveness of the subject method in reducing forces can be clearly shown for the three examples through a comparison of elevator control forces per unit acceleration with and without aerodynamic balance. The values are 50, 80, and 600 with a radius balance nose in comparison with values of 20, 30, and 110 which can be obtained with reasonable values of aerodynamic balance.

Control Effectiveness

In order to provide adequate control effectiveness, particularly at low air speeds, without an excess of movable surface area, it is considered best to use the highest allowable movable control surface angle consistent with a continuous increase in lift. This design consideration materially affects the choice of aerodynamic balance, since it is evident from the basic wind-tunnel data that for a given hinge-moment reduction the blunt-nose-shaped balance causes premature stall, while the sharp-nose-shaped balance gives hinge-moment reversal at high angles. The tendency to stall off the control surface nose at high angles is greatly affected by the surface angle of attack. At $\alpha = 0°$, for example, as in the case of a rudder on a twin-engined airplane after engine failure when trimmed for zero sideslip, the stall occurs much earlier than when the angle of attack of the surface is opposed to the flap deflection as in the case of an elevator during landing or the rudder in a sideslip. This difference usually limits the amount of aerodynamic balance which can be used on a rudder in comparison with that on an elevator.

In order to illustrate further the effects of this consideration on the choice of aerodynamic balance, curves of hinge moment and lift characteristics vs. control surface angle were analyzed from the basic data. The point at which the movable surface stalled was taken as that where either an abrupt increase in hinge moment or a break in lift occurred. Results of this study are given in Figs. 13a and 13b in the form of stall boundaries, limiting the values of elevator aerodynamic balance for the particular case of a horizontal surface in the landing attitude, $\alpha = 10°$. A comparison of these figures indicates a required reduction in aerodynamic balance as the maximum up-travel of the elevator is in-

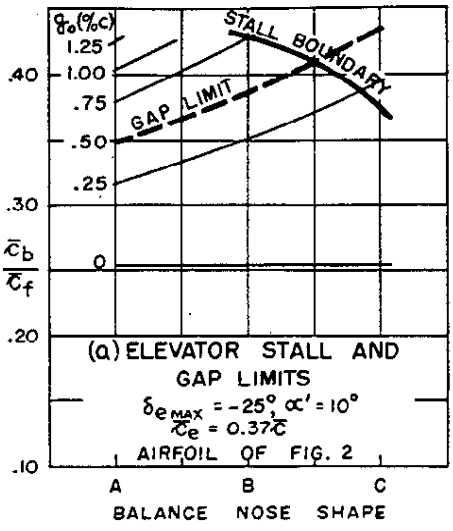

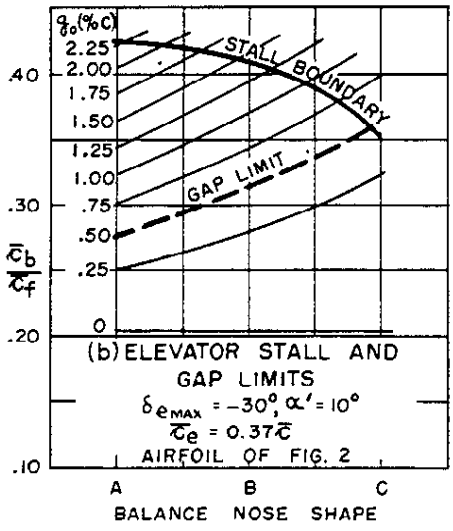

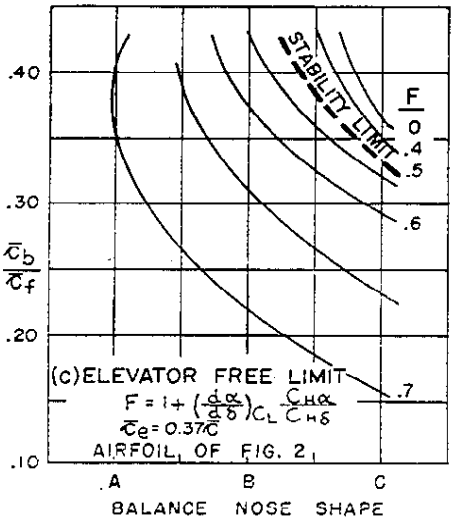

FIG. 13. Practical design limits applicable to elevator aerodynamic balance and nose shape.

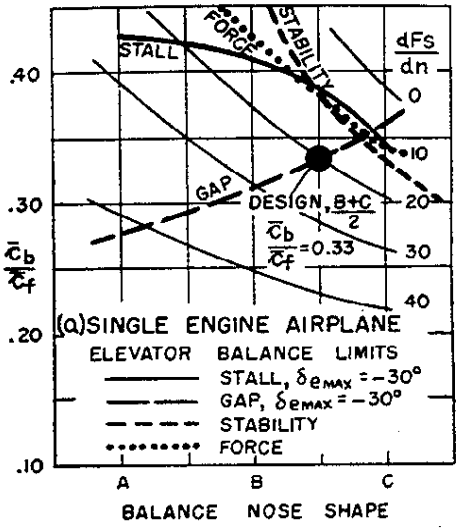

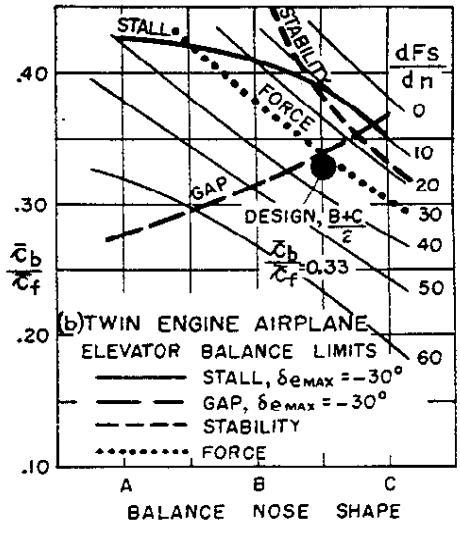

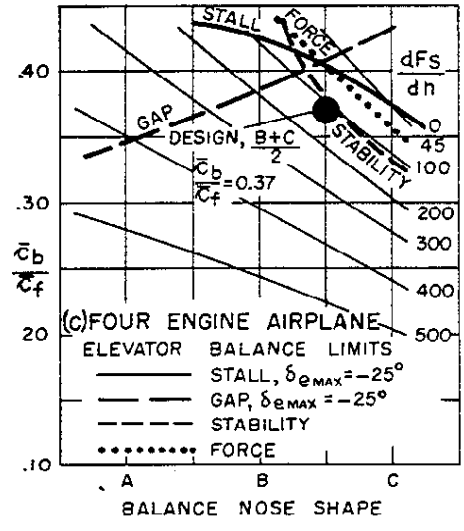

FIG. 14. Application of aerodynamic balance limits to representative airplanes showing relationship to elevator stick force per unit normal acceleration and recommended aerodynamic balance.

creased ($\delta_{emax.}$ from $-25°$ to $-30°$). Although advantage may sometimes be taken of less maximum elevator travel to effect a stick-force reduction through resulting increase in mechanical advantage as well as through increased aerodynamic balance, other design considerations usually demand that all available control surface effectiveness from angular throw be obtained.

Overtravel Gap

If a control surface is deflected beyond a certain angle, unporting of the nose leading edge outside the airfoil contour will be sufficient to cause a sudden hinge-moment reversal, particularly when the angle of attack on the surface opposes that of the control. This brings another consideration into the picture, the amount of allowable overtravel gap (g_0). Whereas with a sharp-nose shape and high balance overhang, maximum throw will be severely limited by this consideration, a blunt-nose shape with less overhang will permit more angular travel. Although no quantitative data are available to establish a gap limit, design experience indicates that the value of g_0 should be taken as $\leqq 0.50$ per cent c for satisfactory hinge-moment characteristics at full movable surface throw. The relationship of this limit to variation in balance overhang and nose shape is shown for the case of an elevator in Figs. 13a and 13b for limiting travels of $\delta_{emax.} = -25°$ and $-30°$. It is apparent from these figures that a fixed value of overtravel gap limits particularly the amount of overhang which can be used as balance nose shape is sharpened.

It is possible to increase the allowable overtravel gap by the use of a fabric seal between fixed and movable surfaces in cases where maximum control effectiveness has not been obtained. Here the difficulty of designing and manufacturing a satisfactory seal must be compared with the aerodynamic advantages gained. These will be discussed later in the paper. In order to prevent exceeding the limiting angular travel of a control surface once the allowable value of overtravel gap has been chosen, it is imperative that stops be furnished at the control surface rather than in the cockpit.

Free-Control Stability

A further consideration bearing directly upon the choice of aerodynamic balance is the degree to which control-free stability is adversely affected. The ratio of free- to fixed-control stability due to tail surfaces only may be expressed as

$$F = 1 + (d\alpha/d\delta)c_L(C_{H_\alpha}/C_{H_\delta}) \qquad (11)$$

The variation of F with aerodynamic balance is shown in Fig. 13c, where a pronounced decrease in free-control stability is evident with hinge-moment reduction. The factor, F, decreases both as the balance nose shape is changed from sharp to blunt and as the amount of balance overhang is increased. This loss in free-control stability with proportional balance overhang must be considered during the initial stages of control surface design in relation to the advantages of control-force reduction. For the study of balance limits applicable to an elevator (Fig. 14) a value of $F = 0.5$ was chosen to represent the maximum loss in free-control longitudinal stability which could be exchanged for desirable control force reduction on a large airplane. This limit is closely approached in the case of the four-engined airplane (Fig. 14c) where a high degree of hinge-moment reduction is required to bring control forces within the fixed limit of pilot strength.

Icing

Another factor entering into the design of a movable control surface is the degree to which the balance nose is subject to critical ice formation. The results of the Goodrich icing tests shown in Fig. 7 indicate that formations of a critical nature can form on the various balance noses, particularly at high control surface angles. For example, with $\delta_f = 20°$ the ice formations on all nose shapes with 35 per cent balance are such that the control surface probably could not be returned to neutral. In order to evaluate the degree to which the various noses are subject to icing, the angle, β, was measured for all cases. A purely qualitative inspection indicates that when this angle is greater than 135° a critical condition will probably result. Upon this basis the limiting control surface angles shown in Fig. 15 for balance overhang and nose-shape variations were obtained.

The primary instance where icing possibilities must be avoided is in the case of the rudder of a multiengined airplane. After failure of an engine, the asymmetric thrust must be trimmed out for a considerable length of time well within the limits for critical ice formation to occur. In designing the rudder for such a case it is necessary that the effectiveness be adequate to trim for the most critical engine failure condition with a rudder angle such that $\beta \leqq 135°$. Using representative two- and four-engined airplane designs with rudders having the (B + C)/2 nose-shape and balance overhang values of 0.28 and 0.33, respectively, the rudder angles

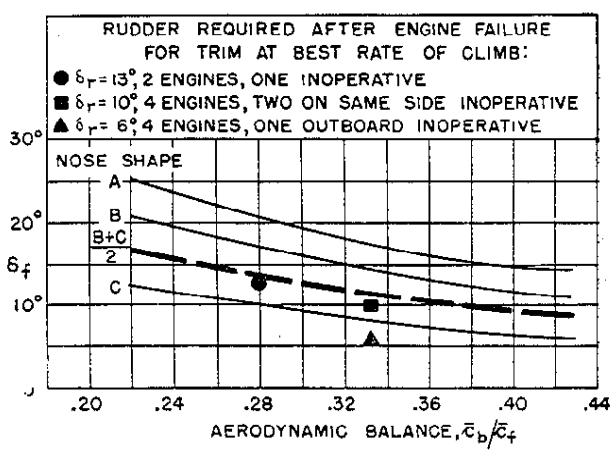

FIG. 15. Limiting control surface angles for acrodynamic balance and nose shape variations to avoid undesirable ice formation. Control surface angles determined on basis of $\beta = 135°$. [Examples are with (B + C)/2 nose shape.]

for various conditions of engine failure are shown in Fig. 15. Although the twin-engined case after failure of one engine is the most critical, the rudder effectiveness has been chosen such that δ_r does not exceed the icing limit. Because the rudder in the case of the four-engined airplane was necessarily designed for the critical condition of two engines inoperative on the same side, ample margin exists for the more usual case of only one outboard engine inoperative ($\delta_r = 6°$).

Effect of Modifications

Although the factors given in Fig. 9 specifically apply only to control surfaces having the NACA 0012 section modified to 10.7 per cent c thickness by 12 per cent c extension with flat-sided afterbody and with hinge line at 63 per cent c, design applications have indicated that the data presented may be used with reasonable approximation for cases varying from the above airfoil section. Since application of these data to other cases must be accompanied by good judgment and the full realization of possible errors, a brief discussion is included treating the effects of various modifications and their relative merits based principally upon Douglas testing and design experience.

Airfoil Section

Reasons for selecting the NACA 0012 airfoil as the basic section have already been discussed. Other than leading edge radius, which exerts a powerful influence upon the stalling characteristics, the most important airfoil section properties that may be altered are the maximum thickness and chordwise location of maximum thickness. For a control surface without aerodynamic balance, increasing the thickness or moving the maximum ordinate aft will generally reduce the factors η_α, η_δ, and η_λ. The principal effect of these changes is to increase the included angle at the trailing edge with resulting decrease in circulation and alteration in pressure distribution, particularly over the movable control surface afterbody. From DC-2 flight tests and later model tests, changes in airfoil contour forward of the movable surface appear to have minor effects on control surface parameters. It is reasonable to expect, however, that the effects of viscosity will become more pronounced as airfoil thickness is increased, making it necessary to interpret carefully wind-tunnel results on thicker surfaces.

For an aerodynamically balanced surface the above reductions in factors η_α, η_δ, and η_λ are partially offset by a decrease in balance effectiveness. Increasing the thickness of the balance nose section, whether by moving the maximum ordinate aft or by increasing airfoil thickness, reduces the amount of balance which will project outside the airfoil contour for a given δ_f, with the inevitable result that the balancing pressures are reduced. Thus, Fig. 9 cannot be used to calculate accurately the effects of change in balance overhang or nose shape for airfoil sections of different thickness ratio or distribution. Since, however, the loss in balance effectiveness is offset by a corresponding reduction in the factors for an unbalanced surface, it is considered that the use of Fig. 9 for estimating hinge moments on other airfoils can be used for a rough first approximation in the absence of more specific data on the correct airfoil section.

In general, the use of airfoil sections of maximum thickness greater than 12 per cent c is not recommended for control surface design, primarily because the thicker sections indicate a greater tendency to develop "flat spots" in the hinge moment vs. angle curve near neutral, particularly when the control surface is subject to the seemingly inevitable manufacturing irregularities that move the transition point forward. For a limited range of angle of attack and control surface deflection, C_{H_α} may become positive and C_{H_δ} extremely small. With control system friction, the floating tendency of a control surface having this combination of parameters may give rise to objectionable oscillations.

Afterbody Shape

Considerable variation in the hinge-moment parameters of a control surface may be obtained through

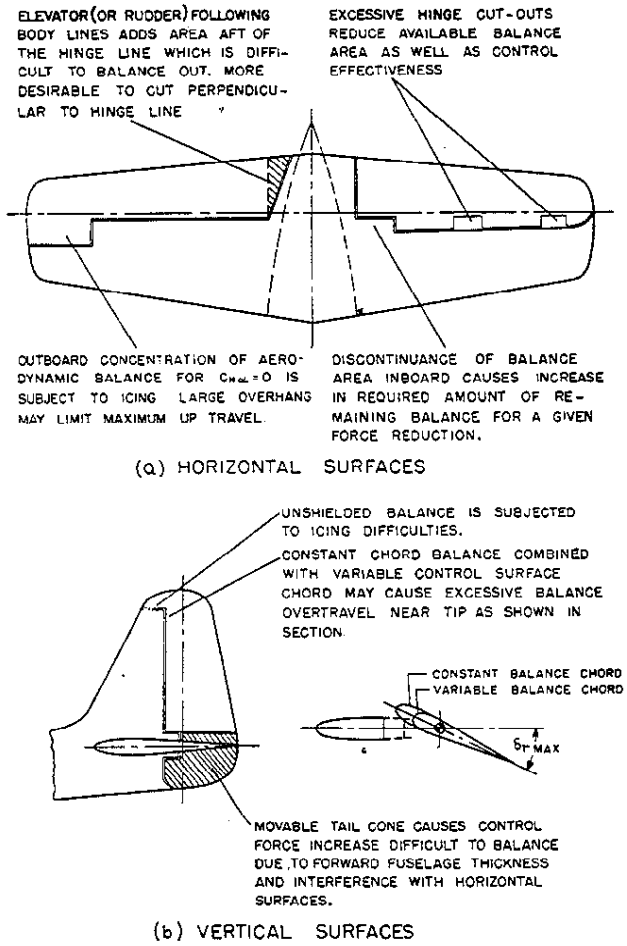

Fig. 16. Design features to be avoided for maximum aerodynamic balance efficiency.

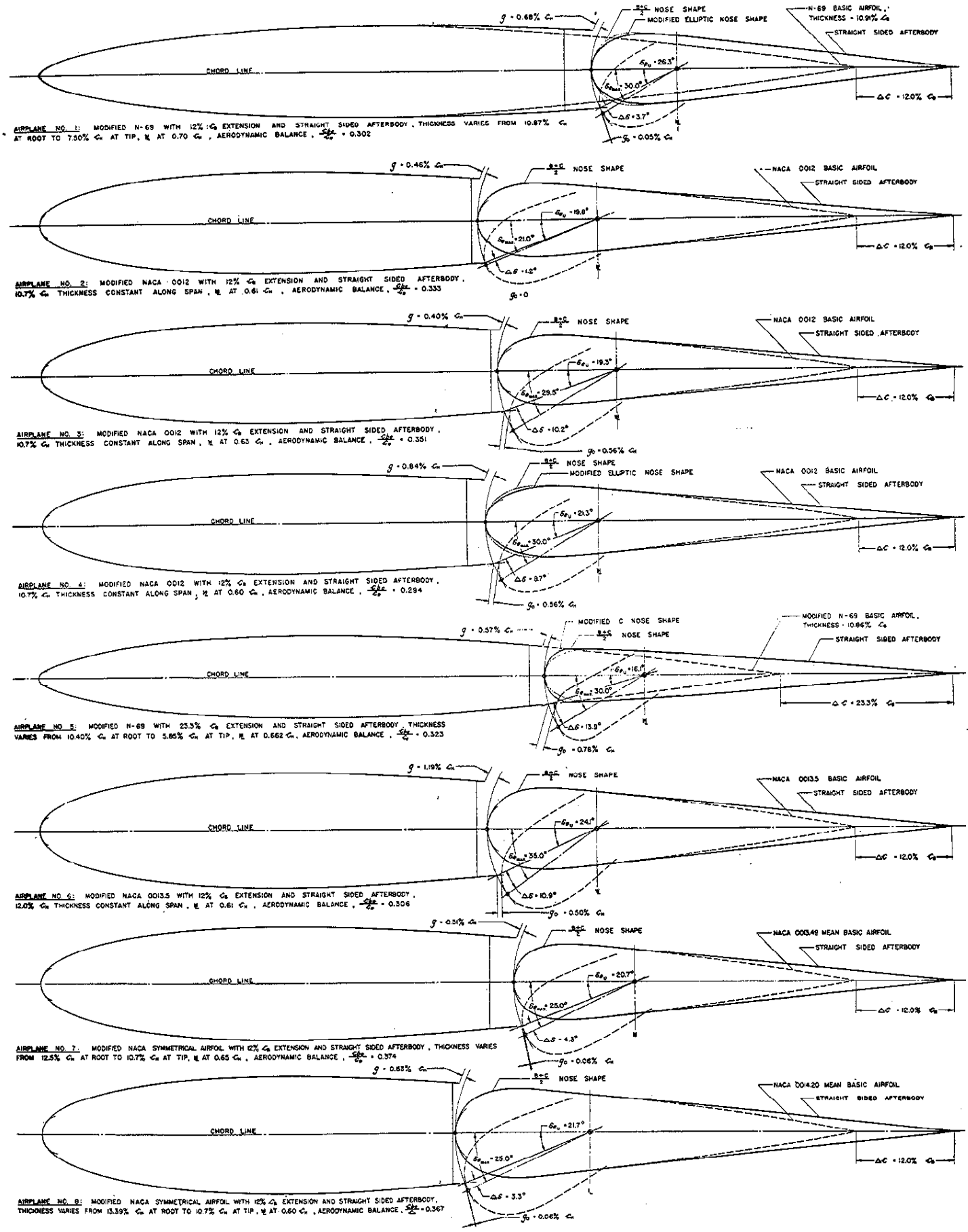

FIG. 17. Representative horizontal surface mean airfoil sections from a number of full-scale airplanes upon which elevator aerodynamic balancing has been successfully employed.

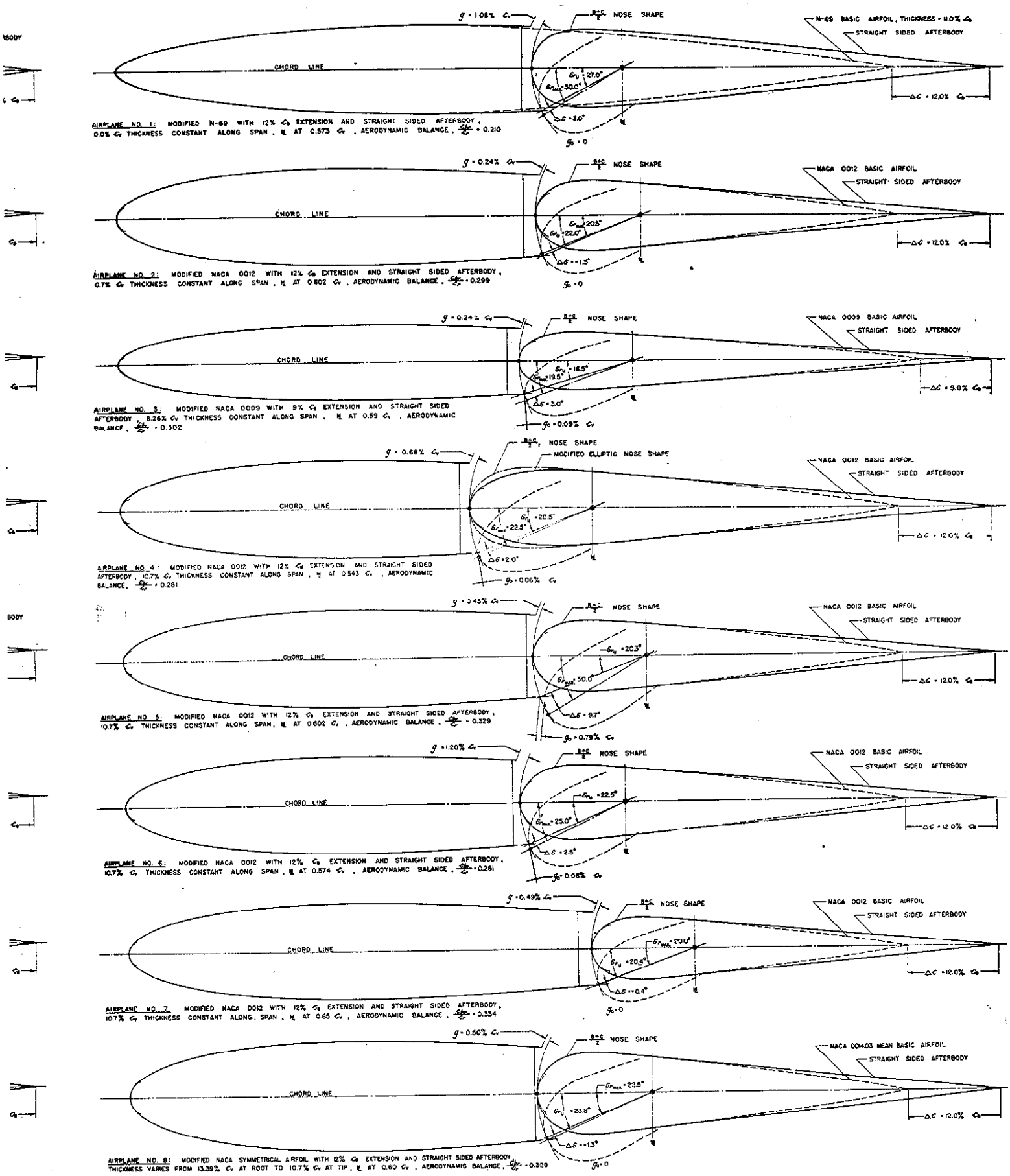

ic bal-

FIG. 18. Representative vertical surface mean airfoil sections from a number of full-scale airplanes upon which rudder aerodynamic balancing has been successfully employed.

alteration of afterbody shape. Data in Fig. 9 are specifically applicable to flat-sided control surfaces having a trailing edge angle of 10° and therefore cannot be applied with any degree of accuracy to control surfaces with afterbodies convexed, concaved, thickened, bevelled, or stripped. In general, any modification that increases the trailing edge angle will decrease η_α, η_δ, and η_λ as in the case of an increase in thickness. Although a convex-sided afterbody may be effectively used to change hinge-moment parameters, particularly to reduce C_{H_α}, a movable control surface with this shape is considered more susceptible to undesirable oscillations and to a loss in control "feel" through neutral.

Hinge Location

The empiric correction factors, η_α, η_δ, and η_λ, are used in conjunction with the theoretic parameters of Fig. 10 to permit a variation in movable surface per cent chord to be taken into account in obtaining the parameters, $(dc_h/dc_l)_\delta$, $(dc_h/d\delta)_{cl}$, and $(d\alpha/d\delta)_{cl}$. As c_f/c is varied, a change in aerodynamic balance effectiveness is to be expected, since the thickness in the region of the balance nose is altered with hinge-line relocation. Since test points shown in Fig. 12 for scale models do not show any consistent trend within the range of hinge locations tested, it is believed that the present method can be used without appreciable error for $\Delta c_f/c = \pm 0.04$. Rudder and elevator hinge lines used on conventional designs will probably lie within this range.

Gaps and Seals

In addition to permitting an acceptable increase in rudder or elevator angular travel, sealing the gap between a fixed and movable control surface offers a method of increasing the fixed-control stability through an increase in C_{L_α}. This increase, however, is usually obtained at the expense of a corresponding hinge-moment increase as illustrated in the auxiliary graph of Fig. 9. Here the effect of reducing control surface gap (g) is shown for (B + C)/2 nose shape and 33 per cent aerodynamic balance. Factors η_α and η_λ are not affected by gap size within the accuracy of the basic test data. The empiric factor, η_δ, however, was increased from 0.39 to 0.49 with gap change from 0.5 per cent c to a complete seal. For the horizontal surface of the single-engined example previously used, these changes amount to increases in elevator stick force per unit acceleration from 20 to 30 in exchange for an approximate 2 per cent M.A.C. rearward movement of the fixed-control longitudinal stability neutral point. Presumably some of this increase in stick force could be overcome through use of a smaller tail surface in the initial design stage. Loss in lift curve slope, C_{L_α}, would be expected to increase with larger gaps and with forward chordwise movement of gap location into a lower pressure region.

Influence on Design

For maximum aerodynamic balance efficiency it is considered advisable to use proportional control surface

TABLE III

HORIZONTAL SURFACE SECTION CHARACTERISTICS

Airplane Number	AIRFOIL SECTION: Basic Airfoil Type	Basic Airfoil Root	Basic Airfoil Tip	Chord Extension (% c_B)	Thickness (% c): Root	Thickness (% c): Tip	Trailing Edge: Included Angle (deg.)	Trailing Edge: Radius (% c)	ELEVATOR: Hinge Location $\bar{x}_e/\bar{c}_H$	Aerodynamic Balance $\bar{c}_{b_e}/\bar{c}_e$	Nose Shape	Angles (Degrees): Design Stops $\delta_{e\ max.}$°	L.E. Unporting δ_{e_U}°	Over Travel Δ_{δ}°	Icing Limit $\delta_{e\ ice}$°	Gaps (% c): Minimum Clearance g	Over Travel g_o
1	N-69	12.17	8.40	12	10.87	7.50	13.7	0.12	0.300	0.302	Modified Elliptic	-30 + 20	26.3	3.7	16.0	0.68	0.05
2	NACA	0012	0012	12	10.7	10.7	10.1	0.06	0.390	0.333	B+C/2	-21 + 18	19.8	1.2	11.7	0.46	0
3	NACA	0012	0012	12	10.7	10.7	10.1	0.12	0.370	0.351	B+C/2	-29.5 + 11.75	19.3	10.2	10.7	0.40	0.56
4	NACA	0012	0012	12	10.7	10.7	10.1	0.10	0.400	0.294	Modified Elliptic	-30 + 20	21.3	8.7	14.8	0.84	0.56
5	N-69	11.10	9.32	23.3	10.40	5.85	9.2	0.08	0.338	0.323	Modified C	-30 + 20	16.1	13.9	4.5	0.57	0.78
6	NACA	0013.5	0013.5	12	12.0	12.0	11.3	0.07	0.390	0.306	B+C/2	-35 + 20	24.1	10.9	14.7	1.29	0.50
7	NACA	0014	0012	12	12.5	10.7	11.3	0.15	0.350	0.374	B+C/2	-25 + 15	20.7	4.3	10.7	0.51	0.06
8	NACA	0015	0012	12	13.39	10.7	11.8	0.10	0.400	0.367	B+C/2	-25 + 20	21.7	3.3	11.3	0.53	0.06

TABLE IV

VERTICAL SURFACE SECTION CHARACTERISTICS

Airplane Number	AIRFOIL SECTION: Basic Airfoil Type	Basic Airfoil Root	Basic Airfoil Tip	Chord Extension (% c_B)	Thickness (% c): Root	Thickness (% c): Tip	Trailing Edge: Included Angle (deg.)	Trailing Edge: Radius (% c)	RUDDER: Hinge Location $\bar{x}_r/\bar{c}_v$	Aerodynamic Balance $\bar{c}_{b_r}/\bar{c}_r$	Nose Shape	Angles (Degrees): Design Stops $\delta_{r\ max.}$°	L.E. Unporting δ_{r_U}°	Over Travel Δ_{δ}°	Icing Limit $\delta_{r\ ice}$°	Gaps (% c): Minimum Clearance g	Over Travel g_o
1	N-69	11.20	11.20	12	10.0	10.0	11.7	0.12	0.427	0.210	B+C/2	±30	27.0	3.0	16.0	1.08	0
2	NACA	0012	0012	12	10.7	10.7	10.1	0.06	0.398	0.299	B+C/2	±20.5	22.0	-1.5	13.7	0.24	0
3	NACA	0009	0009	9	8.26	8.26	8.2	0.17	0.410	0.302	B+C/2	±19.5	16.5	3.0	10.0	0.24	0.09
4	NACA	0012	0012	12	10.7	10.7	10.1	0.07	0.457	0.281	Modified Elliptic	±22.5	20.5	2.0	15.7	0.68	0.06
5	NACA	0012	0012	12	10.7	10.7	10.1	0.14	0.398	0.329	B+C/2	±30	20.3	9.7	11.9	0.43	0.79
6	NACA	0012	0012	12	10.7	10.7	10.1	0.06	0.426	0.281	B+C/2	±25	22.5	2.5	13.7	1.20	0.06
7	NACA	0012	0012	12	10.7	10.7	10.1	0.13	0.350	0.334	B+C/2	±20	20.4	-0.4	11.0	0.49	0
8	NACA	0015	0012	12	13.39	10.7	11.8	0.08	0.400	0.328	B+C/2	±22.5	23.8	-1.3	12.9	0.50	0

plan form and section. Since balance overhang can then be chosen as a constant ratio along the span, both the amount of balance required for a given hinge-moment reduction and the overtravel gap can be minimized, thus increasing control effectiveness. To obtain completely uniform angular projection of the balance nose section outside the control surface airfoil contour all along the span, airfoil sections must necessarily be similar. In cases, however, where the root thickness has been increased for structural reasons, balance overhang or nose shape will have to be altered along the span to provide equivalent hinge-moment reduction. Proportionality of both plan form and section not only permits a closer approximation of control surface characteristics to be made from section test data but also provides a major simplification in design layout and lofting processes.

Several horizontal and vertical control surface planform variations to be avoided for maximum balance efficiency are shown in Fig. 16. It is necessary to point out that, although certain of these features have been successfully employed in control surface design, their use will not result in the best solution with respect to satisfying the aerodynamic balance design requirements previously outlined. The degree to which it is necessary to meet these requirements remains directly dependent upon the amount of hinge moment reduction desired without resorting to other means. In this respect an airplane with conventional empennage proportions and a wing area of 1,400 sq.ft. is considered representative of a conservative upper limit beyond which a satisfactory solution to the control force problem using aerodynamic balance alone cannot be expected. For designs above this arbitrary limit, however, conservative aerodynamic balance values can still be used to design advantage as follows: by reducing hinge moments that must be handled by power boost or other means; by providing means for sectional balance weight attachment, thus giving movable surface dynamic as well as static mass balance; by reducing control system loads; and by increasing the control effectiveness of a tab.

As an aid toward the application of the design principles discussed in this paper, the airfoil section characteristics for the horizontal and vertical surfaces of eight Douglas airplanes are presented in Figs. 17 and 18. Quantitative data are listed in Tables III and IV, from which representative variations may be obtained with respect to airfoil section, hinge location, balance over-hang, nose shape, limiting angular travels, and gaps.

References

[1] Jacobs, E. N., Ward, K. E., and Pinkerton, R. M., *The Characteristics of 78 Related Airfoil Sections from Tests in the Variable-Density Wind Tunnel*, N.A.C.A. T.R. No. 460, 1933.

[2] Ames, M. B., Jr., and Sears, R. I., *Determination of Control-Surface Characteristics from NACA Plain-Flap and Tab Data*, N.A.C.A. T.R. No. 721, 1941.

Erratum

In the article "Stress Analysis of Open Cylindrical Membranes" by Leon Beskin (JOURNAL OF THE AERONAUTICAL SCIENCES, Vol. 11, No. 4, p. 343, October, 1944) a mistake occured on page 350, right column, under Eq. (48). The sentence should read: "The coordinates of that point being (x_1, y_1) in respect to the shear center."